ACS Partner Journal

CHEM & BIO ENGINEERING

pubs.acs.org/ChemBioEng

Article

Electrocatalytic Cleavage of C−C Bonds in Lignin Models Using Nonmetallic Catalysts at Ambient Conditions

Guangyong Liu, Ziqi Zhai, Yumiao Lu, JunFeng Lu, Yanlei Wang, Shijing Liang,* Hongyan He,* and Lilong Jiang

Cite This: *Chem Bio Eng.* 2024, 1, 357−365

Read Online

ACCESS | Metrics & More | Article Recommendations | Supporting Information

ABSTRACT: Lignin, characterized by its amorphous, heavily polymerized structure, is a primary natural source of aromatic compounds, yet its complex constitution poses considerable challenges in its transformation and utilization. Therefore, the selective cleavage of C−C bonds represents a critical and challenging step in lignin degradation, essential for the production of high-value aromatic compounds. In this study, we report a simple electrocatalytic approach for lignin valorization via C−C bond cleavage by developing a nonmetallic electrocatalyst of carbon-based materials. It is found that the hydrophilicity and hydrophobicity of the electrocatalyst have a significant effect on the degradation process. Under mild conditions, the hydrophilic carbon paper exhibits 100% substrate conversion, yielding 97% benzaldehyde and 96% quinone with ionic liquid electrolytes. The mechanism study shows that the carbon catalyst with higher surface defects favors electron transfer in the oxidative cleavage process of C−C bonds. These results signify a substantial advancement in lignin degradation, offering an environmentally friendly, metal-free electrochemical route.

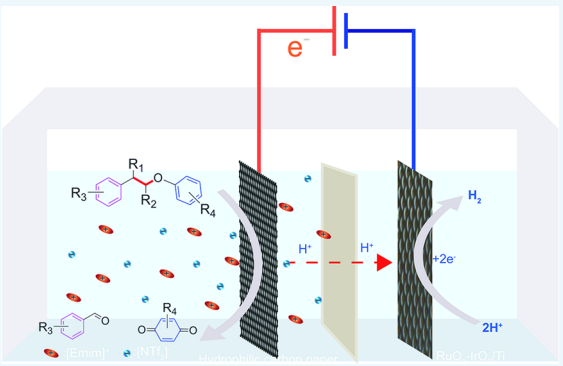

KEYWORDS: *Lignin, Degradation, Nonmetallic electrocatalyst, Hydrophilicity, Ionic liquid*

1. INTRODUCTION

Given the substantial consumption of fossil fuels and their limited storage, there is a pressing need to explore alternative energy and chemical resources.[1,2] Therefore, the development and utilization of renewable bioenergy, particularly lignocellulose, the world's most abundant bioenergy source, has received a great deal of attention. Lignin, a major component of lignocellulosic biomass (15%−30% by weight), emerges as a promising renewable feedstock for the production of alternative fuels, platform compounds, and high-value chemicals.[1−4] However, the low reactivity and market value of lignin result in its underutilization, often being relegated to a byproduct in bioethanol production and pulping industries.[3] Lignin's complex, amorphous polymeric structure, comprising bonds between C−O and C−C units, is formed by the enzymatic dehydrogenation polymerization of phenylpropionic acid monomers (e.g., sinapyl alcohol, conifery alcohol, and p-coumary alcohol), creating linkages like β-O-4, α-O-4, β-5, $\beta-\beta$, 4-O-5, 5-5, and β-1.[1−4] However, its structural complexity and low reactivity lead to a mere 2% utilization rate, with the majority being burned.[5] Therefore, the development of suitable methods to convert lignin into high-value bulk chemicals is particularly important and urgent. Currently, the efficient utilization of lignin remains a significant challenge and a bottleneck in biomass valorization. Existing lignin depolymerization methods, such as oxidation,[6,7] hydrogenolysis,[8,9] pyrolysis,[10,11] catalytic depolymerization,[12,13] and electrolysis,[14,15] each with its own set of challenges and opportunities.

Electrocatalytic degradation of lignin has the advantages of controllable reaction and environmental sustainability, emerging as a promising method for lignin degradation valorization.[16−21] Current research in this area predominantly focuses on electrochemical oxidation at the anode. This involves a variety of materials including transition metals (e.g., Ni, Co),[22] metal alloys (e.g., mixtures of Ni, Co, Fe, Ti),[23] metal oxides (e.g., IrO_2, PbO_2, SnO_2),[24,25] and mixed metal oxide anodes.[26] He et al. reported the depolymerization of ethanol organosolv lignin from different sources using cost-effective nickel foam as the working electrode under alkaline conditions, which achieved a maximum yield of 17.5% for vanillin and syringaldehyde.[27] Furthermore, Duan and Wang et al. explored the electrocatalytic oxidation of C_α-C_β bonds employing Pt atoms dispersed on nitrogen-doped carbon nanotubes (Pt/N-CNTs), achieving an impressive 99% substrate conversion and 81% aldehyde yield.[28] Despite these

Received: December 24, 2023
Revised: February 2, 2024
Accepted: February 13, 2024
Published: February 26, 2024

Scheme 1. Different Strategies of Lignin Depolymerization[28,35]

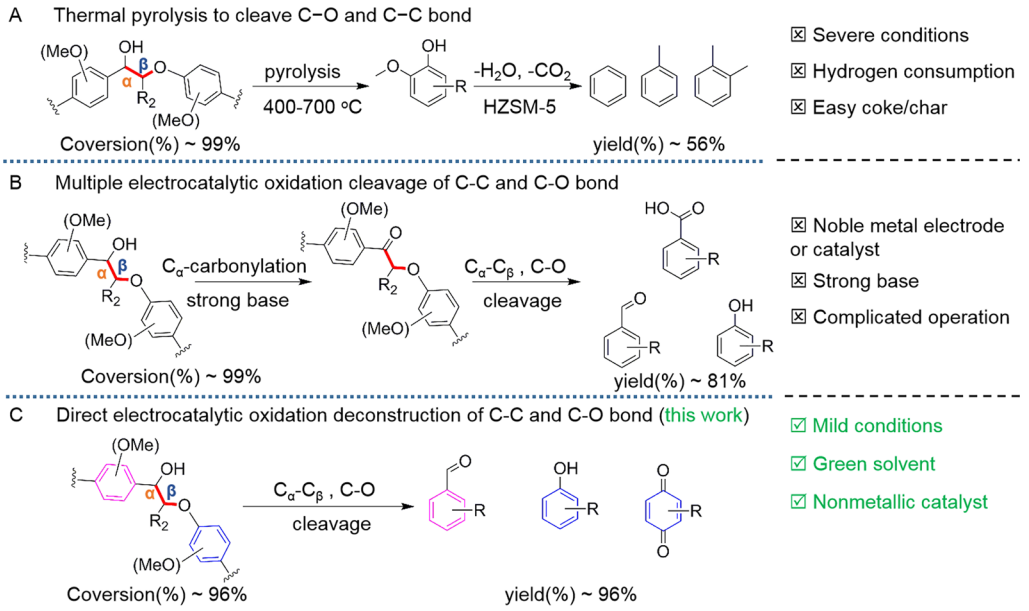

advances, this field still faces challenges such as low yields, poor selectivity, and reliance on noble metals.

Therefore, developing efficient, environmentally benign, and stable electrocatalytic methods for lignin degradation is of paramount importance, particularly considering the challenges associated with lignin's limited solubility in conventional solvents. In this scenario, ionic liquids (ILs) stand out due to their favorable solvation properties for both organic substances and lignin.[4,29,30] At the same time, ILs offer a range of advantages, including wide electrochemical window, non-volatility, high thermal stability, non-flammability, excellent solubility in organic and inorganic substances, coupled with designability, making them promising candidates as electrolytes.[31−34] Consequently, the electrocatalytic decomposition of lignin in ILs has attracted extensive attention in recent research.

Among all types of natural lignin bonds, the β-O-4 bond constitutes the most prevalent linkage in natural lignin (approximately 50%). The dissociation energies of different aliphatic C−O and C−C bonds are 293 and 314−494 kJ mol^{-1}, respectively, indicating a substantial energy requirement for selective C−C bond cleavage.[1−3,7,28] While notable advancements have been made in breaking C_α-O bonds to yield ketones and phenols, research on the selective cleavage of C−C bonds remains largely unexplored. Specifically, the study of electrocatalytic cleavage of C−C bonds in lignin, especially using nonmetallic electrodes in ILs, is still in its infancy and is a promising area of future research.

Building upon existing research, we propose an investigation into the electrocatalytic oxidation of C−C and C−O bonds in lignin model compounds, employing ILs and metal-free electrodes under mild conditions (see Scheme 1).[28,35] This method contrasts with traditional thermal catalysis by avoiding harsh reaction conditions, high temperatures and the need for hydrogen sources. Unlike electrocatalysis employing noble metal electrodes, our approach does not require expensive noble metals or strong alkaline solutions. Herein, we employ carbon electrodes for the electrocatalytic cleavage of C−C and C−O bonds in lignin model compounds dissolved in ILs. Specifically, under optimum conditions, the yield of aldehyde and quinone is as high as 90%, along with the conversion rate exceeding 90%. At the same time, H_2 is produced as a by-product at the counter electrode. These findings suggest a promising, sustainable alternative to conventional lignin degradation methods, with potential implications for green chemistry and renewable resource utilization.

2. EXPERIMENTAL SECTION

2.1. Reagents and Materials. Acetonitrile (MeCN) and methanol (HPLC grade, 99.9%), $KClO_4$ (AR) were obtained from Aladdin Co. Ltd. (Beijing, China). The **1a−1h** substrates and $H_2{}^{18}O$ used in the study were obtained from Macklin Co. Ltd. (Shanghai, China). *N*-Propyl-*N*-methylpyrrolidinium bis(trifluoromethyl sulfonyl)imide ($[Py_{13}][NTf_2]$, 98%), *N*-butyl-*N*-methylpyrrolidinium trifluoromethanesulfonate ($[Py_{13}][OTf]$, 98%), trimethylpropylammonium bis(trifluoromethyl sulfonyl)imide ($[N_{1113}][NTf_2]$, 98%), *N*,*N*-diethylmethylammonium trifluoromethanesulfonate ($[N_{221}][OTf]$, 98%), *N*-ethylimidazolium bis((trifluoromethyl) sulfonyl)imide ($[Emim][NTf_2]$, 98%), and 1-ethyl-3-methylimidazolium tetrafluoroborate ($[Emim][BF_4]$, 98%) ILs were purchased from Qingdao aolike new material technology Co. Ltd. (Qingdao, China). The structures of these ILs are shown in the ESM (Figure S1). Hydrophilic carbon paper (HL cp), carbon fiber cloth (HL cfc) and Hydrophobic carbon paper (HB cp), carbon fiber cloth (HB cfc), Nafion-117 membrane were provided by the Shanghai Chuxi industry Co. Ltd. (Shanghai, China). Deionized water was made in the laboratory. The RuO_2−IrO_2/Ti mesh was provided by the Northwest Institute for Nonferrous Metals Research (Xi'an, China).

2.2. Electrolysis of Lignin Model Compounds. The electrochemical oxidation of lignin model compounds was conducted using a constant potential method on a PARSTAT3000A-DXelectrochemical workstation (Princeton Instruments, Inc., USA). The reaction was carried out in a three-electrode H-cell system with a Nafion-117 membrane. An IL-MeCN solution (14 mL, 0.5 mL H_2O) containing 15 mM lignin model compounds was used in the anode chamber,

https://doi.org/10.1021/cbe.3c00122
Chem Bio Eng. 2024, 1, 357−365

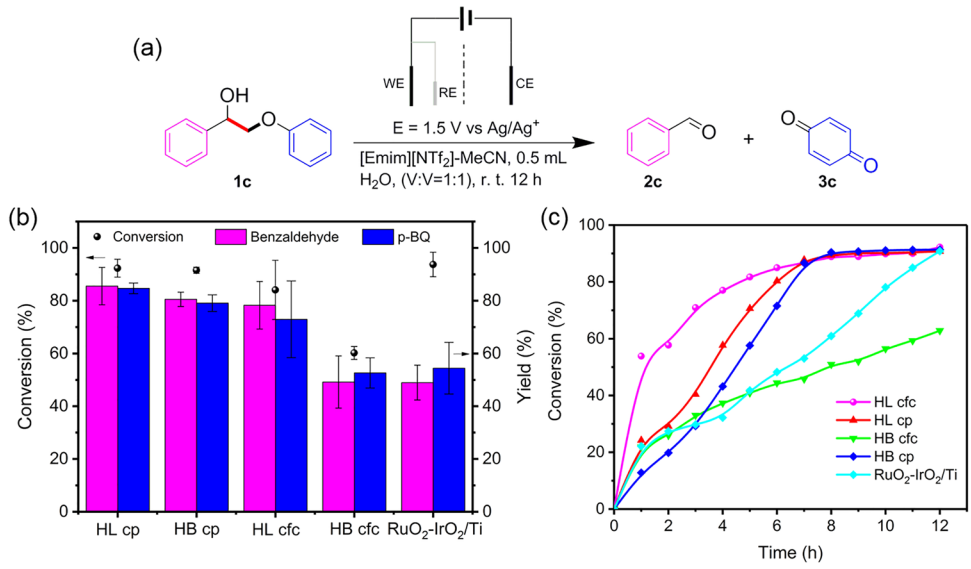

Figure 1. Electrooxidation performance of the anode catalytic system. (a) Electrocatalytic oxidation of the C−C bond of **1c**. (b) Conversion and product yields of **1c** under different catalysts at the same catalytic conditions. (c) Reaction−time curve of **1c** under different catalysts.

while 10 mL of 0.5 M H_2SO_4 solution was used in the cathode chamber. Carbon cloth or paper (~1.2 × 3 cm^2) was used as the working electrode. The counter electrode was RuO_2−IrO_2/Ti of the same size. For reference electrode, we employed an Ag/Ag^+ electrode, consisting of an Ag-wire immersed in 10 mM $AgNO_3$ solution in a glass tube with a porous plug.

2.3. Catalyst Characterization. Morphologies and structures of the nonmetallic carbon electrodes were characterized using a field-emission scanning electron microscope (SEM, model SU8020). The surface composition of the electrodes was analyzed by X-ray photoelectron spectroscopy (XPS) on an ESCALAB 250Xi spectrometer using a 75-150 W Al Kα cathode source under ultrahigh vacuum, and the C 1s line was used to calibrate all raw XPS spectra at 284.80 eV. Raman spectroscopy was performed using an OPTIMA 8000infrared spectrometer (Renishawn). The scanning range is 200−2500 cm^{-1}, the excitation light source is λ = 325 nm, the laser intensity is 1%, the scanning time is 8, and the exposure time is 2−10 s. The Surface contact angle between the nonmetallic carbon electrode and electrolyte was measured by a contact angle measuring instrument (LSA60, LAUDA, Germany).

2.4. GC-MS and HPLC Analysis. Degradation products were analyzed using a gas chromatography coupled with a mass spectrometer (GC-MS, Shimadzu GC-2030). This system was equipped with an Rtx-5MS Ultra Inert capillary column (30 m × 250 μm × 0.25 μm) and an AOC-6000 Plus headspace sampler. For analysis, the samples were first gasified at 170 °C for 1 min, and then injected through headspace, followed by testing with a 10:1 split ratio. Degradation products of lignin model compounds were analyzed by an high-performance liquid chromatography (HPLC, LC-20ADxr) equipped with a SPD-20A UV detector and a C18 column (250 mm × 4.6 mm i.d., 5 μm). The mobile phase consisted of a mixture of methanol and water with a volume ratio of 3:2 or 2:3 (**1h**, GG) at a flow rate of 0.5 mL min^{-1} and a temperature of 35 °C. Quantification of the observed products were carried out at 254 nm using an external standard method. The conversion of lignin model compounds and the yields of products were calculated using the following eqs 1 and 2:

$$\text{conversion}\ (\%) = (C_0 - C_t) \times 100/C_0 \quad (1)$$

$$\text{yield}\ (\%) = C_{\text{products}} \times 100/C_0 \quad (2)$$

where C_0 represents the initial concentration of the lignin model compound, C_t represents the lignin model compound concentration at the sampling time, and C_{products} represents the product concentration.

3. RESULTS AND DISCUSSION

3.1. Electrocatalytic Cleavage of Lignin Dimers. In direct electrooxidation, electrochemical processes mainly occur on the anode surfaces, making the choice of anode material a crucial role in determining the catalytic activity.[21] In this study, we investigated the electrooxidation of lignin model compounds using various commercial electrode materials, including HL cfc, HB cfc, HL cp, HB cp, and RuO_2−IrO_2/Ti (Figure 1), in the presence of the typical IL [Emim][NTf_2] as the electrolyte. As shown in Figure 1b, all five materials can degrade the lignin model compound to varying degrees, and surprisingly, the readily available carbon materials exhibit the same and even superior conversion ratios compared to the noble metal electrode. At the same time, the product yields of four carbon materials are also much higher than that of the noble metal electrode. These results indicate that carbon materials have a significant advantage over noble metals for the electrocatalytic degradation of lignin. The obvious difference in product yields may be attributed to the high electrocatalytic activity of noble metals, which can further oxidize aromatic compounds into carbon dioxide and water.[36] It is worth noting that the main product of benzaldehyde, which can only be produced through C_α−C_β bond cleavage, suggesting the oxidative cleavage ability of the C−C bonds by carbon materials, which is generally thought to be reserved for noble metals.[28] Further examination of the carbon materials reveals differences in their cleavage abilities. Firstly, carbon paper delivers a higher product yield compared to carbon fiber cloth, implying the structural effect of carbon materials on catalytic performance. Secondly, within the same carbon structure, hydrophilic carbons demonstrate a better conversion ratios and

https://doi.org/10.1021/cbe.3c00122
Chem Bio Eng. 2024, 1, 357−365

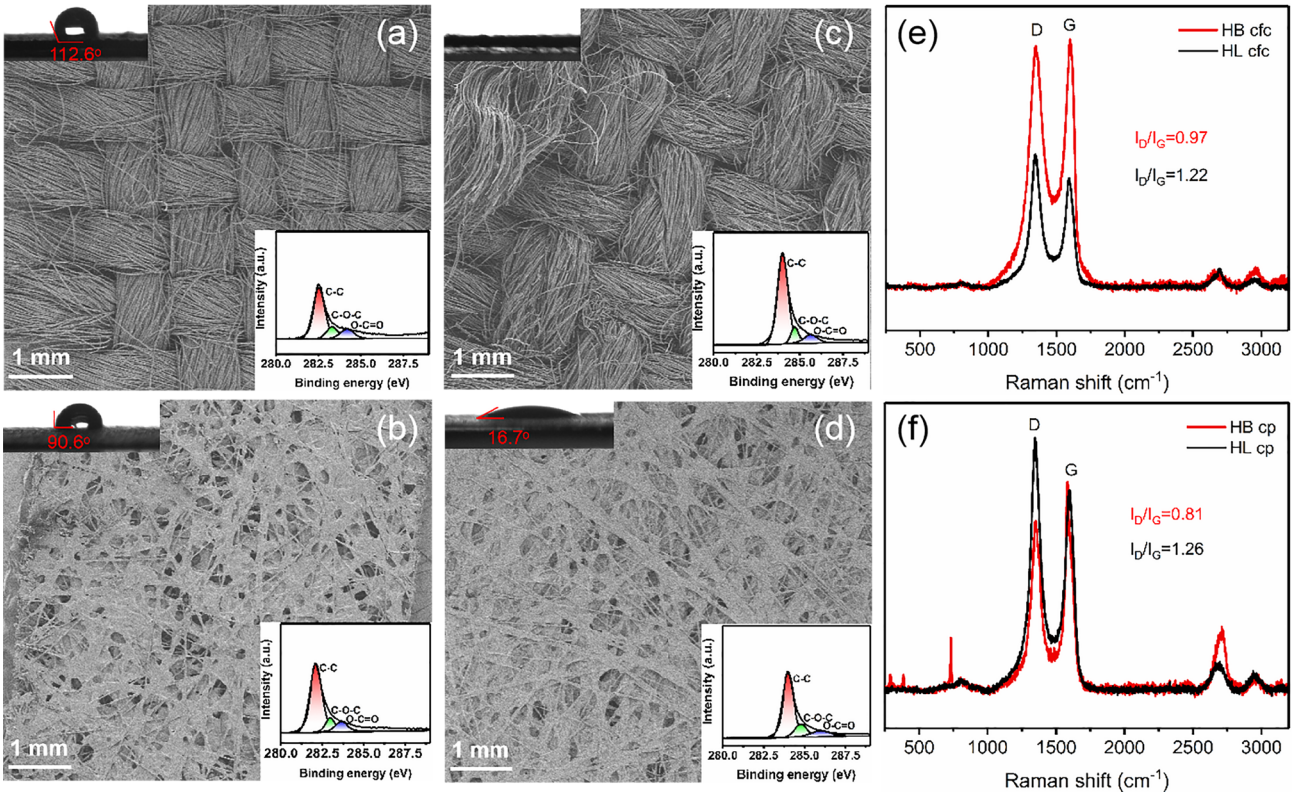

Figure 2. Structural characterization of carbon catalysts. SEM image, contact angle, and high-resolution XPS spectra of C 1s for (a) HB cfc, (b) HB cp, (c) HL cfc, and (d) HL cp. (e,f) Raman spectrogram of HB cfc, HL cfc and HB cp, and HL cp.

product yields than that of hydrophobic carbons, suggesting the surface chemistry effect on the catalytic process. Based on the reaction-time curves (Figure 1c), it can be seen that the HL cfc exhibits the highest degradation rate in the first 6 h, which further proves the better catalytic feature among hydrophilic carbons. With time increasing, HL cp, HL cfc, and HB cp can achieve the same substrate conversion ratio after 8 h, indicating that time is an essential factor in evaluating the catalytic performance.

3.2. Carbon Materials Characterization. In order to gain insight into the catalytic difference among various carbon materials, we performed SEM, Raman, XPS, and contact angle characterizations (Figure 2). SEM images show that all four kinds of carbon materials are composed of carbon nanorods (Figure S2). The major difference lies in surface morphology, with cfc exhibiting regular woven mesh structure, whereas cp has a large specific surface area due to the presence of micropores (Figure 2a–d). The increased specific surface area is advantageous for exposing more active sites, thereby enhancing its catalytic activity. Considering the hydrophilic effect in the degradation experiments, we performed the contact angle experiments using electrolytes to mimic the real reaction interface between the electrode and electrolyte. Principally, good wettability of electrolytes on the electrode can promote the electrocatalytic reaction, and vice versa. As expected, the wettability of HL cp and HL cfc is better than that of HB cp and HB cfc, which explains the enhanced degradation efficiency (Figure 1b). The wetting behavior is usually related to the surface chemistry of materials, and thus XPS and Raman characterizations were employed. The spectra of C 1s show the presence of C–C, C–O–C, and O–C=O bonds,[37,38] indicating the existence of oxygenic functional groups on the surface of these carbon materials. To quantify the oxygen content, the peak area ratios of C–C, C–O–C, and O–C=O bonds of HL cp, HL cfc, HB cp, and HB cfc were calculated, which are 1:0.16:0.11, 1:0.16:0.10, 1:0.13:0.12, and 1:0.12:0.05. These results demonstrate that HL cp and HL cfc have significantly higher levels of oxygenic functional groups compared to HB cfc. To further confirm the surface chemistry feature of the carbon materials, we conducted Raman characterizations (Figures 2e and f), which exhibit typical D-band and G-band peaks at 1348 and 1598 cm^{-1}, respectively. Based on prior studies, the D-band is associated with the defects in carbon, while the G-band arises from the graphitic carbon phase.[38] The intensity ratio of D-band to G-band (I_D/I_G) can be used to quantify the defect level in carbon materials.[39,40] The calculated I_D/I_G values for the four carbon materials are 1.26 (HL cp) > 1.22 (HL cfc) > 0.97 (HB cp) > 0.81 (HB cfc). According to the literature, higher levels of structure defects induces changes in electronic structure and energy bands, thus giving carbon materials more active sites in electrocatalytic reactions.[41,42] Therefore, the different hydrophilicity and activity defects of carbon materials contribute to variations in the electrocatalytic degradation performance. Specifically, HL cp, characterized by better hydrophilicity and a higher level of activity defects, should exhibit the best activity for the electrocatalytic degradation of **1c**, which is consistent with our experimental finding in Section 3.1. Based on these results, HL cp was selected as the electrode material for catalytic reactions in the following study.

3.3. Electrocatalytic Study. The successful cleavage of the C–C bond demonstrates the potential application of ILs as electrolytes, offering a viable alternative to alkaline solutions in lignin depolymerization.[16,29–31,43–45] To identify more suitable

https://doi.org/10.1021/cbe.3c00122
Chem Bio Eng. 2024, 1, 357–365

Table 1. Electrooxidation Results of 1c with Different IL-MeCN Electrolytes[a]

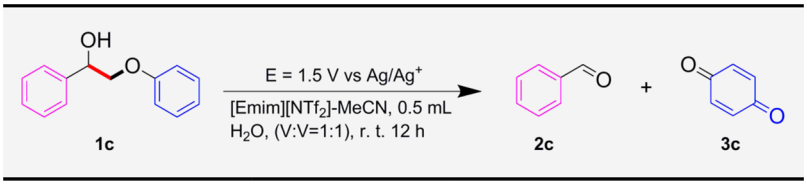

entry	conversion 1c (%)	yield 2c (%)	yield 3c (%)
[Emim][NTf_2]-MeCN	90.77	86.81	80.28
[Py_{13}][NTf_2]-MeCN	91.42	81.07	80.16
[N_{1113}][NTf_2]-MeCN	92.06	84.57	79.29
[Py_{13}][OTf]-MeCN	98.67	61.11	78.04
[N_{221}][OTf]-MeCN	88.49	75.56	73.48
[Emim][BF_4]-MeCN	88.20	74.48	72.80
MeCN(Saturated $KClO_4$)	83.35	48.74	77.85

[a]Reaction conditions: ILs-MeCN (V:V=1:1) with 15 mM 1c, cathode electrolyte (0.5 M H_2SO_4), divided cell, constant potential control.

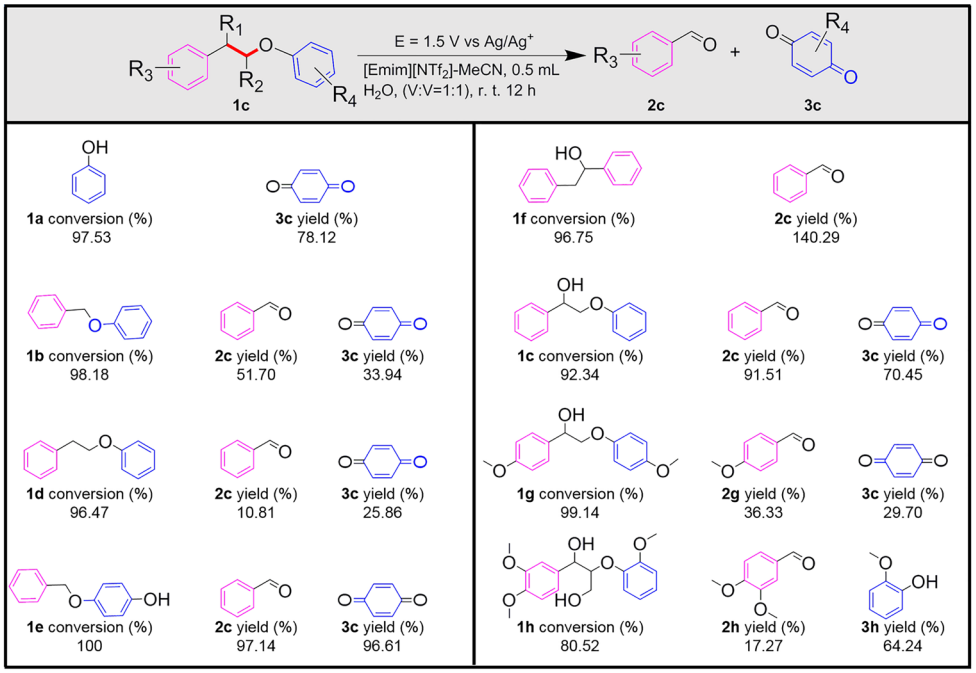

Figure 3. Electrocatalytic oxidation of different lignin model compounds.

types of ILs, different combinations of cations and anions were employed to perform the electrochemical depolymerization experiments, as summarized in Table 1. Acetonitrile (MeCN) was chosen due to its compatibility with lignin dissolution and its capacity to reduce electrolyte viscosity, thus enhancing conductivity. Encouragingly, these ILs exhibit better conversion ratios and product yields compared to the inorganic salt solution. Among the six systems evaluated, [Emim][NTf_2], [Py_{13}][NTf_2], [N_{1113}][NTf_2] and [Py_{13}][OTf] show higher conversion rates exceeding 90%, while [Emim][BF_4] exhibits the lowest conversion. An examination of viscosity and conductivity of the electrolyte systems shows that the conversion of 1c decreases with the increase of electrolyte viscosity (Table S1). That's because the higher viscosity restricts the efficiency of ion transport and further slows down the electrocatalytic reaction. Consequently, the higher viscosity of the [Emim][BF_4] system results in a lower conversion ratio. Despite the much lower viscosity of saturated $KClO_4$-MeCN solution compared to ILs, its ultra-low conductivity leads to the lowest conversion ratio.

Another important observation is the influence of ILs on product yield. It can be seen that anions tend to affect the product yield compared to cations, with [NTf_2]$^-$ facilitating the highest yield of aldehyde and quinone. Even when [Emim]-[BF_4] and [Emim][NTf_2] ILs exhibit similar conversion rates for 1c, the product yields still increase from 74.48% and 72.80% to 86.8% and 80.2%, respectively. In other words, [NTf_2]$^-$ creates a more favorable environment for stabilizing the products, possibly owing to its size and charge density.[44] In addition, according to previous study, the strong electronegativity of [NTf_2]$^-$ facilitates electron delocalization between C_β–H bonds, thus promoting the cleavage of C–C bonds and product yield.[45,46] Given the higher conversion and product yield achieved with the [Emim][NTf_2]-MeCN system, we selected it for further study.

Besides the IL structure, several factors, including volume ratio of electrolytes, electrode potential, and substrate

https://doi.org/10.1021/cbe.3c00122
Chem Bio Eng. 2024, 1, 357−365

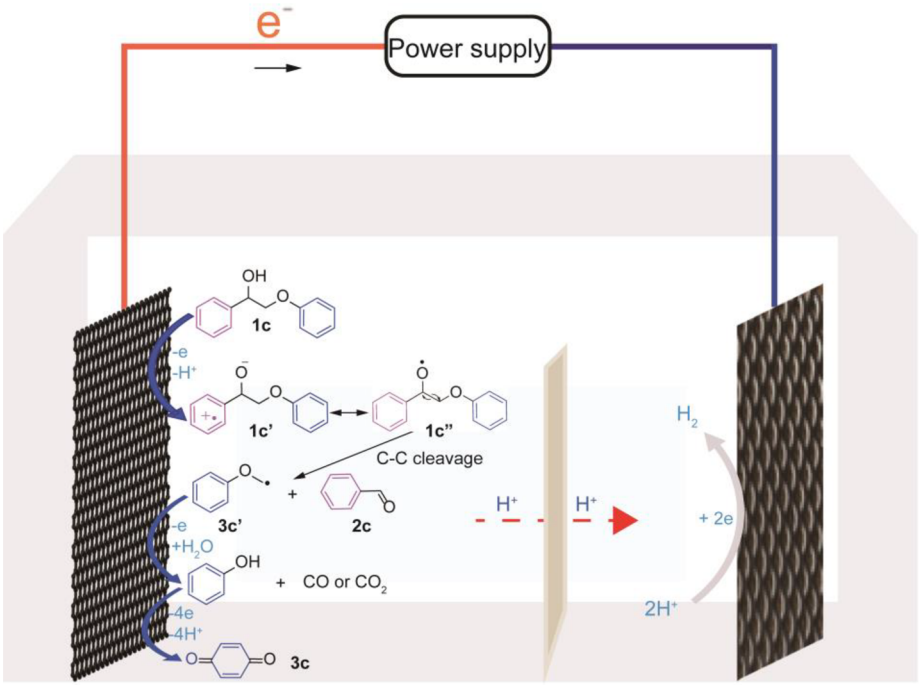

Figure 4. Electrocatalytic oxidation mechanism with carbon catalysts and IL electrolyte.

concentration, also affect the catalytic depolymerization of lignin. Inspired by this, a series of optimization experiments were carried out. As previously discussed, the conductivity of electrolytes is closely correlated with the conversion ratio, we modulated the proportion of ILs dissolved in MeCN. When pure IL is used as the electrolyte, only 20% substrate conversion and 15% and 8% product yields can be achieved. However, with the increase of MeCN volume, both substrate conversion and product yield first increase and then decrease slightly, reaching their peak at an equal volume mixing (Figure S4a). This result can be explained by the changes in viscosity and conductivity at different IL concentrations (Table S2).[44] Compared to the volume ratios of electrolytes, the electrode potential has a more significant impact on lignin depolymerization. The CV curve recorded on glassy carbon electrode (GCE) with 20 mM 1c has an obvious oxidation peak at 1.5 V, which corresponds to the oxidative cleavage of lignin dimers (Figure S5). Therefore, potential-controlled electrolysis of **1c** was explored at potentials of 1.0, 1.5, and 2.0 V (Figure S4b). With increasing potential, the conversion exhibits an upgoing trend from 19.7% to 100%, while the product yield increases first and then decreases. At the high potential of 2.0 V, not only can **1c** be electrocatalytically degraded, but the product would be further oxidized to small molecules,[36] explaining the decreased product yield at high potentials. Therefore, an optimal potential is beneficial to optimize the depolymerization performance and ensuring electrolyte stability, as ILs can remain stable only within a specific electrochemical window (Figures S6-7). Another critical factor is the concentration of the substrate. At high concentrations, the substrate can overcover the catalyst surface, blocking the reaction. Conversely, at low concentrations, the reaction efficiency drops due to the underutilization of the active sites. Based on our experiments, the conversion rate is nearly 95% within the concentration range of 5−25 mM, then the product yield decreases slightly beyond this range (Figure S4c).

3.4. Substrate Scoping. To expand the scope of this protocol, we evaluated various lignin α-O-4, β-O-4, and C_α-C_β dimers (**1a**−**1h**) with different substituents under the optimized conditions (Figure 3). The conversion ratio of **1a**−**1g** is above 90%, but the presence of greater steric hindrance of 1h leads to a lower conversion ratio. The main products of lignin model compounds degradation are the phenol, aldehydes and quinone (Figure S8-15). Notably, the successful degradation of **1f** to aldehyde further demonstrates that the nonmetallic carbon catalyst has the ability to break the C_α-C_β bond in lignin. For **1b**−**1e** and **1g**, the degradation products of aldehydes and quinones prove the breaking of both the C_α-C_β and β-O-4 bonds of substrates during the degradation process. The product of p-benzoquinone suggests the conversion of phenol into quinone, a process easily oxidizable from phenol, as confirmed in our study on the electrocatalytic oxidation of phenol (**1a**), where a high yield of p-benzoquinone was indeed detected, in agreement with previous studies.[47,48] Comparing **1b** and **1e**, we observed that when hydroxyl groups are substituted on the phenol ring (**1e**), the substrate conversion is nearly 100% and the product yield of *p*-benzoquinone is as high as 96%. That's because the presence of hydroxyl group makes the addition of oxygen to the benzene unnecessary, which reduces reaction steps and hence improves efficiency. Similarly, comparing **1c** and **1d**, we found that hydroxyl substitution on C_a can also promote the product yield. Similar to **1b** and **1e**, the cleavage of C−C bond in **1c** results in the generation of phenylacetaldehyde in one step, avoiding multistep oxidation processes.[28,49] These results indicate that the substitution of hydroxyl groups on the phenol ring or C_a can promote substrate degradation and product formation by reducing reaction steps. For substrates **1g** and **1h**, which feature increasingly complicated substituents, the product yields are significantly reduced due to greater steric hindrance.

3.5. Electrocatalytic Oxidation Mechanism. Based on the above experimental results, we put forward the electro-

https://doi.org/10.1021/cbe.3c00122
Chem Bio Eng. 2024, 1, 357−365

catalytic degradation mechanism, as shown in Figure 4. First, compound **1c** loses an electron at the HL cp electrode, while C_a−OH loses a proton (H^+) to form the intermediate **1c′**. The rearrangement of electrons on the C_a-O bond to form **1c″** results in the splitting of the C−C bond to produce phenoxy ether radical (**3c′**) and aldehyde (**2c**).[50,51] Then phenoxy ether radical **3c′** undergoes further oxidization to produce phenol and small molecules such as CO or CO_2.[28,48] Subsequently, phenol loses four electrons and is further oxidized to p-benzoquinone (**3c**) (Figure S16).[47,48] To verify the source of oxygen in *p*-benzoquinone, an oxygen isotope labeling experiment was carried out using $H_2{}^{18}O$ as the electrolyte. The results show that p-benzoquinone has the mass-to-charge ratio of 108 and 110 when both H_2O and $H_2{}^{18}O$ are added to the electrolytic system (Figure S17). It means that the carbon atom of phenol can combine with the hydroxyl group of H_2O to form p-benzoquinone (**3c**). Furthermore, free radical scavenger experiments were also performed and it demonstrates that the presence of Tert-butyl alcohol in the electrolyte significantly slows down the degradation process, which supports the proposed free radical mechanism (Figure S18). As for the lignin dimers without hydroxyl substitution on C_a position, such as **1d** and **1e**, the electrocatalytic mechanism involves the oxidation of either the phenol ring or the phenolic hydroxyl group, leading to the cleavage of the C−O bond (Figures S19 and S20).

4. CONCLUSION

In summary, the mild cleavage of C−C bonds of lignin model compounds has been achieved by constructing an electrocatalytic oxidation system consisting of carbon-based catalysts and IL electrolyte. It was revealed that the hydrophilicity and hydrophobicity of the carbon catalysts had a great influence on the degradation performance, with hydrophilic carbon paper demonstrating optimal performance. The study also identified the optimum reaction conditions under which different lignin dimers could be completely degraded via C−C and C−O bond cleavage. Based on the degradation mechanism, we found that the presence of hydroxyl groups on the phenol ring or at the C_a position can promote substrate degradation and enhance product yield by reducing reaction steps. Overall, these findings point new insights into catalyst design for lignin depolymerization and provide a fundamental understanding of lignin depolymerization.

■ ASSOCIATED CONTENT

Supporting Information

The Supporting Information is available free of charge at https://pubs.acs.org/doi/10.1021/cbe.3c00122.

Additional experimental characterization of the carbon catalysts and electrolytes; structures of the ILs and degradation mechanism (PDF)

■ AUTHOR INFORMATION

Corresponding Authors

Shijing Liang − *National Engineering Research Center of Chemical Fertilizer Catalyst, Fuzhou University, Fuzhou 350002 Fujian, China*; Email: sjliang2012@fzu.edu.cn

Hongyan He − *CAS Key Laboratory of Green Process and Engineering, State Key Laboratory of Multiphase Complex Systems, Beijing Key Laboratory of Ionic Liquids Clean Process, Institute of Process Engineering, Chinese Academy of Sciences, Beijing 100190, China; Longzihu New Energy Laboratory, Zhengzhou Institute of Emerging Industrial Technology, Zhengzhou 450000, China*; orcid.org/0000-0003-1291-2771; Email: hyhe@ipe.ac.cn

Authors

Guangyong Liu − *National Engineering Research Center of Chemical Fertilizer Catalyst, Fuzhou University, Fuzhou 350002 Fujian, China; CAS Key Laboratory of Green Process and Engineering, State Key Laboratory of Multiphase Complex Systems, Beijing Key Laboratory of Ionic Liquids Clean Process, Institute of Process Engineering, Chinese Academy of Sciences, Beijing 100190, China*

Ziqi Zhai − *CAS Key Laboratory of Green Process and Engineering, State Key Laboratory of Multiphase Complex Systems, Beijing Key Laboratory of Ionic Liquids Clean Process, Institute of Process Engineering, Chinese Academy of Sciences, Beijing 100190, China*

Yumiao Lu − *CAS Key Laboratory of Green Process and Engineering, State Key Laboratory of Multiphase Complex Systems, Beijing Key Laboratory of Ionic Liquids Clean Process, Institute of Process Engineering, Chinese Academy of Sciences, Beijing 100190, China*

JunFeng Lu − *CAS Key Laboratory of Green Process and Engineering, State Key Laboratory of Multiphase Complex Systems, Beijing Key Laboratory of Ionic Liquids Clean Process, Institute of Process Engineering, Chinese Academy of Sciences, Beijing 100190, China*

Yanlei Wang − *CAS Key Laboratory of Green Process and Engineering, State Key Laboratory of Multiphase Complex Systems, Beijing Key Laboratory of Ionic Liquids Clean Process, Institute of Process Engineering, Chinese Academy of Sciences, Beijing 100190, China; Longzihu New Energy Laboratory, Zhengzhou Institute of Emerging Industrial Technology, Zhengzhou 450000, China*; orcid.org/0000-0002-2214-8781

Lilong Jiang − *National Engineering Research Center of Chemical Fertilizer Catalyst, Fuzhou University, Fuzhou 350002 Fujian, China*; orcid.org/0000-0002-0081-0367

Complete contact information is available at: https://pubs.acs.org/10.1021/cbe.3c00122

Author Contributions

H. Y. He and S. J. Liang designed the experiment; G. Y. Liu performed the experiment; Z. Q. Zhai, Y. M. Lu, J. F. Lu, Y. L. and Wang, L. L. Jiang analyzed the data; H. Y. He, S. J. Liang, and Y. M. Lu wrote the paper; all authors contributed to the discussion of the results.

Notes

The authors declare no competing financial interest.

■ ACKNOWLEDGMENTS

This work was supported by the National Key Research and Development Program of China (2021YFB3802600), the National Natural Science Foundation of China (22278396, 22378392, 22178344), the Youth Innovation Promotion Association CAS (Y2021022), and the Open Research Fund of State Key Laboratory of Mesoscience and Engineering (MESO-23-D17).

REFERENCES

(1) Zhang, Z. R.; Song, J. L.; Han, B. X. Catalytic transformation of lignocellulose into chemicals and fuel products in ionic liquids. *Chem. Rev.* **2017**, *117*, 6834−6880.

(2) Li, C. Z.; Zhao, X. C.; Wang, A. Q.; Huber, G. W.; Zhang, T. Catalytic transformation of lignin for the production of chemicals and fuels. *Chem. Rev.* **2015**, *115*, 11559−11624.

(3) Tuck, C. O.; Pérez, E.; Horváth, I. T.; Sheldon, R. A.; Poliakoff, M. Valorization of biomass: deriving more value from waste. *Science* **2012**, *337*, 695−699.

(4) Zhai, Z. Q.; Lu, Y. M.; Liu, G. Y.; Ding, W. L.; Cao, B. B.; He, H. Y. Recent Advances in Biomass-derived Porous Carbon Materials: Synthesis, Composition and Applications. *Chem. Res. Chin. Univ.* **2024**, *40*, 3−19.

(5) Chatel, G.; Rogers, R. D. Review: oxidation of lignin using ionic liquids-an innovative strategy to produce renewable chemicals. *ACS Sustain. Chem. Eng.* **2014**, *2*, 322−339.

(6) Yu, X. N.; Wei, Z. Q.; Lu, Z. X.; Pei, H. S.; Wang, H. L. Activation of lignin by selective oxidation: An emerging strategy for boosting lignin depolymerization to aromatics. *Bioresource Technol.* **2019**, *291*, No. 121885.

(7) Du, X.; Tricker, A. W.; Yang, W. S.; Katahira, R.; Liu, W.; Kwok, T. T.; Gogoi, P.; Deng, Y. L. Oxidative catalytic fractionation and depolymerization of lignin in a one-pot single-catalyst system. *ACS Sustain. Chem. Eng.* **2021**, *9*, 7719−7727.

(8) Wang, S. Z.; Zhang, K. L.; Li, H. L.; Xiao, L. P.; Song, G. Y. Selective hydrogenolysis of catechyl lignin into propenylcatechol over an atomically dispersed ruthenium catalyst. *Nat. Commun.* **2021**, *12*, 416.

(9) Shen, X. J.; Zhang, C. F.; Han, B. X.; Wang, F. Catalytic self-transfer hydrogenolysis of lignin with endogenous hydrogen: road to the carbon-neutral future. *Chem. Soc. Rev.* **2022**, *51*, 1608−1628.

(10) Leng, E. W.; Guo, Y. L.; Chen, J. W.; Liu, S.; E, J. Q.; Xue, Y. A comprehensive review on lignin pyrolysis: Mechanism, modeling and the effects of inherent metals in biomass. *Fuel* **2022**, *309*, No. 122102.

(11) Rollag, S. A.; Jeong, K.; Peterson, C. A.; Kim, K. H.; Brown, R. C. An experimental and modeling study on the catalytic effects of select metals on the fast pyrolysis of hardwood and softwood lignin. *Green Chem.* **2022**, *24*, 6189−6199.

(12) Zhang, Y. Q.; He, H. Y.; Liu, Y. R.; Wang, Y. L.; Huo, F.; Fan, M. H.; Adidharma, H.; Li, X. H.; Zhang, S. J. Recent progress in theoretical and computational studies on the utilization of lignocellulosic materials. *Green Chem.* **2019**, *21*, 9−35.

(13) Chen, M. Q.; Tang, Z. Y.; Wang, Y. S.; Shi, J. J.; Li, C.; Yang, Z. L.; Wang, J. Catalytic depolymerization of Kraft lignin to liquid fuels and guaiacol over phosphorus modified Mo/Sepiolite catalyst. *Chem. Eng. J.* **2022**, *427*, No. 131761.

(14) Wu, K. J.; Cao, M. L.; Zeng, Q.; Li, X. H. Radical and (photo) electron transfer induced mechanisms for lignin photo-and electro-catalytic depolymerization. *Green Energy Environ.* **2023**, *8*, 383−405.

(15) Caravaca, A.; Garcia-Lorefice, W. E.; Gil, S.; de Lucas-Consuegra, A.; Vernoux, P. Towards a sustainable technology for H_2 production: Direct lignin electrolysis in a continuous-flow Polymer Electrolyte Membrane reactor. *Electrochem. Commun.* **2019**, *100*, 43−47.

(16) Liu, J. C.; Wan, J. P.; Liu, Y. Y. Electrochemical difunctionalization of alkenes and alkynes for the synthesis of organochalcogens involving C-S/Se bond formation. *Org. Chem. Front.* **2024**, *11*, 597−630.

(17) Zhang, C.; Chen, D. M.; Wan, J. P.; Liu, Y. Y. Recent advances in electrochemical cascade cyclization reactions. *Synthesis* **2023**, *55*, 2911−2925.

(18) Guo, H. J.; Liu, Y. Y.; Wan, J. P. Electrochemical cascade pyrazole annulation and C-H halogenation for the synthesis of 4-halopyrazoles. *Green Synth. Catal.* **2023**, DOI: 10.1016/j.gresc.2023.10.004.

(19) Mitsudo, K.; Tachibana, Y.; Sato, E.; Suga, S. Electrochemical synthesis of dibenzothiophenes via intramolecular C-S cyclization with a halogen mediator. *Org. Lett.* **2022**, *24*, 8547−8552.

(20) Guo, H. J.; Liu, Y. Y.; Wen, C. P.; Wan, J. P. Electrochemical enaminone C-H thiolation/C-N amination cascade for thiazole synthesis and its diastereoselective dearomatization. *Green Chem.* **2022**, *24*, 5058−5063.

(21) Du, X.; Zhang, H. C.; Sullivan, K. P.; Gogoi, P.; Deng, Y. L. Electrochemical lignin conversion. *ChemSusChem* **2020**, *13*, 4318−4343.

(22) Zirbes, M.; Schmitt, D.; Beiser, N.; Pitton, D.; Hoffmann, T.; Waldvogel, S. R. Anodic degradation of lignin at active transition metal-based alloys and performance-enhanced anodes. *ChemElectroChem.* **2019**, *6*, 155−161.

(23) Tolba, R.; Tian, M.; Wen, J.; Jiang, Z. H.; Chen, A. Z. Electrochemical oxidation of lignin at IrO_2-based oxide electrodes. *J. Electroanal. Chem.* **2010**, *649*, 9−15.

(24) Shao, D.; Liang, J. D.; Cui, X. M.; Xu, H.; Yan, W. Electrochemical oxidation of lignin by two typical electrodes: Ti/$SbSnO_2$ and Ti/PbO_2. *Chem. Eng. J.* **2014**, *244*, 288−295.

(25) Chen, J.; Yang, H. L.; Fu, H. Q.; He, H. Y.; Zeng, Q.; Li, X. H. Electrochemical oxidation mechanisms for selective products due to C−O and C−C cleavages of β-O-4 linkages in lignin model compounds. *Phys. Chem. Chem. Phys.* **2020**, *22*, 11508−11518.

(26) Yan, K. L.; Zhang, Y.; Tu, M. B.; Sun, Y. J. Electrocatalytic valorization of organosolv lignin utilizing a nickel-based electrocatalyst. *Energy Fuels* **2020**, *34*, 12703−12709.

(27) Liu, G. Y.; Wang, Q.; Yan, D. X.; Zhang, Y. Q.; Wang, C. L.; Liang, S. J.; Jiang, L. L.; He, H. Y. Insights into the electrochemical degradation of phenolic lignin model compounds in a protic ionic liquid−water system. *Green Chem.* **2021**, *23*, 1665−1677.

(28) Cui, T. T.; Ma, L. N.; Wang, S. B.; Ye, C. L.; Liang, X.; Zhang, Z. D.; Meng, G.; Zheng, L. R.; Hu, H. S.; Zhang, J. W.; Duan, H. H.; Wang, D. S.; Li, Y. D. Atomically dispersed Pt-N_3C_1 sites enabling efficient and selective electrocatalytic C-C bond cleavage in lignin models under ambient conditions. *J. Am. Chem. Soc.* **2021**, *143*, 9429−9439.

(29) Liang, L.; Yan, J. P.; He, Q.; Luong, T.; Pray, T. R.; Simmons, B. A.; Sun, N. Scale-up of biomass conversion using 1-ethyl-3-methylimidazolium acetate as the solvent. *Green Energy Environ.* **2019**, *4*, 432−438.

(30) Li, Z. M.; Cai, Z. P.; Zeng, Q.; Zhang, T.; France, L. J.; Song, C. H.; Zhang, Y. Q.; He, H. Y.; Jiang, L. L.; Long, J. X.; Li, X. H. Selective catalytic tailoring of the H unit in herbaceous lignin for methyl p-hydroxycinnamate production over metal-based ionic liquids. *Green Chem.* **2018**, *20*, 3743−3752.

(31) Wang, Y. C.; Wang, S. S.; Liu, L. L. Recovery of natural active molecules using aqueous two-phase systems comprising of ionic liquids/deep eutectic solvents. *Green Chem. Eng.* **2022**, *3*, 5−14.

(32) Liang, L.; Yan, J. P.; He, Q.; Luong, T.; Pray, T. R.; Simmons, B. A.; Sun, N. Scale-up of biomass conversion using 1-ethyl-3-methylimidazolium acetate as the solvent. *Green Energy Environ.* **2019**, *4*, 432−438.

(33) Sun, W. Z.; Wang, M. C.; Zhang, Y. Q.; Ding, W. L.; Huo, F.; Wei, L.; He, H. Y. Protic vs aprotic ionic liquid for CO_2 fixation: a simulation study. *Green Energy Environ.* **2020**, *5*, 183−194.

(34) Stiefel, S.; Marks, C.; Schmidt, T.; Hanisch, S.; Spalding, G.; Wessling, M. Overcoming lignin heterogeneity: reliably characterizing the cleavage of technical lignin. *Green Chem.* **2016**, *18*, 531−540.

(35) Zhang, C. F.; Li, H. J.; Lu, J. M.; Zhang, X. C.; MacArthur, K. E.; Heggen, M.; Wang, F. Promoting lignin depolymerization and restraining the condensation via an oxidation-hydrogenation strategy. *ACS Catal.* **2017**, *7*, 3419−3429.

(36) Bock, C.; MacDougall, B. The anodic oxidation of p-Benzoquinone and maleic acid. *J. Electrochem. Soc.* **1999**, *146*, 2925.

(37) Chen, X. N.; Wang, X. H.; Fang, D. A review on C1s XPS-spectra for some kinds of carbon materials. *Fuller. Nanotub. Car. N.* **2020**, *28*, 1048−1058.

(38) Fang, D.; He, F.; Xie, J. L.; Xue, L. H. Calibration of binding energy positions with C1s for XPS results. *J. Wuhan Univ. Technol.* **2020**, *35*, 711−718.

https://doi.org/10.1021/cbe.3c00122
Chem Bio Eng. 2024, 1, 357−365

(39) Zhou, J.; Yang, P.; Kots, P. A.; Cohen, M.; Chen, Y.; Quinn, C. M.; Vlachos, D. G.; et al. Tuning the reactivity of carbon surfaces with oxygen-containing functional groups. *Nat. Commun.* **2023**, *14*, 2293.
(40) Li, Z. J.; Li, H.; Li, M.; Hu, J. R.; Liu, Y. Y.; Sun, D. M.; Fu, G. T.; Tang, Y. W. Iminodiacetonitrile induce-synthesis of two-dimensional PdNi/Ni@ carbon nanosheets with uniform dispersion and strong interface bonding as an effective bifunctional eletrocatalyst in air-cathode. *Energy Storage Mater.* **2021**, *42*, 118−128.
(41) Yan, D. F.; Li, Y. X.; Huo, J.; Chen, R.; Dai, L. M.; Wang, S. Y. Defect chemistry of nonprecious-metal electrocatalysts for oxygen reactions. *Adv. Mater.* **2017**, *29*, No. 1606459.
(42) Zhu, J. W.; Mu, S. C. Defect engineering in carbon-based electrocatalysts: insight into intrinsic carbon defects. *Adv. Funct. Mater.* **2020**, *30*, No. 2001097.
(43) Liu, G. Y.; Lu, Y. M.; Lu, J. F.; Wang, Y. L.; Liang, S. J.; He, H. Y.; Jiang, L. L. Ionic liquid-trimetallic electrocatalytic system for C-O bond cleavage in lignin model compounds and lignin under ambient conditions. *Nano Res.* **2023**, DOI: 10.1007/s12274-023-6086-z.
(44) Loyson, P.; Imrie, C.; Gouws, S.; Barton, B.; Kruger, E. Bmim ionic liquids as media for the electrochemical oxidation of 2,6-di-t-butylphenol. *J. Appl. Electrochem.* **2009**, *39*, 1087−1095.
(45) Yang, Y. Y.; Fan, H. L.; Song, J. L.; Meng, Q. L.; Zhou, H. C.; Wu, L. Q.; Yang, G. Y.; Han, B. X. Free radical reaction promoted by ionic liquid: a route for metal-free oxidation depolymerization of lignin model compound and lignin. *Chem. Commun.* **2015**, *51*, 4028−4031.
(46) Kang, Y.; Lu, X. M.; Zhang, G. J.; Yao, X. Q.; Xin, J. Y.; Yang, S. Q.; Yang, Y. Q.; Xu, J. L.; Feng, M.; Zhang, S. J. Metal-Free Photochemical degradation of lignin-derived aryl ethers and lignin by autologous radicals through ionic liquid induction. *ChemSusChem* **2019**, *12*, 4005−4013.
(47) Enache, T. A.; Oliveira-Brett, A. M. Phenol and para-substituted phenols electrochemical oxidation pathways. *J. Electroanaly. Chem.* **2011**, *655*, 9−16.
(48) Wu, R. Z.; Meng, Q. L.; Yan, J.; Liu, H. Z.; Zhu, Q. G.; Zheng, L. R.; Zhang, J.; Han, B. X. Electrochemical strategy for the simultaneous production of cyclohexanone and benzoquinone by the reaction of phenol and water. *J. Am. Chem. Soc.* **2022**, *144*, 1556−1571.
(49) Ma, L. N.; Zhou, H.; Kong, X. G.; Li, Z. H.; Duan, H. H. An electrocatalytic strategy for C-C bond cleavage in lignin model compounds and lignin under ambient conditions. *ACS Sustain. Chem. Eng.* **2021**, *9*, 1932−1940.
(50) Weinberg, D. R.; Gagliardi, C. J.; Hull, J. F.; Murphy, C. F.; Kent, C. A.; Westlake, B. C.; Paul, A.; Ess, D. H.; McCafferty, D. G.; Meyer, T. J. Proton-coupled electron transfer. *Chem. Rev.* **2012**, *112*, 4016−4093.
(51) Shiraishi, T.; Takano, T.; Kamitakahara, H.; Nakatsubo, F. Studies on electrooxidation of lignin and lignin model compounds. Part 1: Direct electrooxidation of non-phenolic lignin model compounds. *Holzforschung* **2012**, *66*, 303−309.

https://doi.org/10.1021/cbe.3c00122
Chem Bio Eng. 2024, 1, 357−365